Published for SISSA by Springer

Received: October 29, 2015
Revised: February 8, 2016
Accepted: March 29, 2016
Published: April 8, 2016

CP violating Two-Higgs-Doublet Model: constraints and LHC predictions

Venus Keus,[a,b] Stephen F. King,[b] Stefano Moretti[b,c] and Kei Yagyu[b]

[a] *Department of Physics and Helsinki Institute of Physics, University of Helsinki, Gustaf Hallstromin katu 2, FIN-00014, Finland*
[b] *School of Physics and Astronomy, University of Southampton, Southampton, SO17 1BJ, U.K.*
[c] *Particle Physics Department, Rutherford Appleton Laboratory, Chilton, Didcot, Oxon OX11 0QX, U.K.*

E-mail: venus.keus@helsinki.fi, king@soton.ac.uk, s.moretti@soton.ac.uk, k.yagyu@soton.ac.uk

Abstract: Two-Higgs-Doublet Models (2HDMs) are amongst the simplest extensions of the Standard Model. Such models allow for tree-level CP Violation (CPV) in the Higgs sector. We analyse a class of CPV 2HDM (of Type-I) in which only one of the two Higgs doublets couples to quarks and leptons, avoiding dangerous Flavour Changing Neutral Currents. We provide an up to date and comprehensive analysis of the constraints and Large Hadron Collider (LHC) predictions of such a model. Of immediate interest to the LHC Run 2 is the golden channel where all three neutral Higgs bosons are observed to decay into gauge boson pairs, WW and ZZ, providing a smoking gun signature of the CPV 2HDM.

Keywords: Beyond Standard Model, CP violation, Higgs Physics

ArXiv ePrint: 1510.04028

doi:10.1007/JHEP04(2016)048

JHEP04(2016)048

Contents

1 Introduction

The Standard Model (SM) contains one Higgs doublet which is responsible for Electro-Weak Symmetry Breaking (EWSB). The corresponding Higgs boson, with a mass of $\approx 125\,\text{GeV}$, was discovered in 2012 by the ATLAS and CMS experiments at the Large Hadron Collider (LHC) [1, 2]. Although its properties agree so far with the predictions of the SM, including EW Precision Data (EWPD), it remains an intriguing possibility that the observed Higgs boson, denoted here as h, may just be one member of an extended Higgs sector. A good motivation for such an extended Higgs sector is the fact that it allows for a new source of CP Violation (CPV), as required to explain the matter-antimatter asymmetry of the Universe. Sakharov discovered that CPV is a necessary condition for matter-antimatter asymmetry generation [3] and it was later shown that CPV in the SM is insufficient for this purpose [4].

Among the simplest Higgs extensions are the Two-Higgs-Doublet Models (2HDMs), wherein the SM is extended with one extra Higgs doublet with the same quantum numbers as the SM one. CP Conserving (CPC) 2HDMs have been studied in detail in the literature [5–7]. With the introduction of an extra Higgs doublet to which fermions can couple, one encounters the risk of introducing Flavour Changing Neutral Currents (FCNCs) at tree level, which are tightly constrained by experiment. However, these dangerous FCNCs can be avoided by imposing a Z_2 symmetry on the scalar potential and assigning Z_2 charges to the fermions. Under this setup, there are four independent types of Yukawa interactions which are the so-called Type-I, Type-II, Type-X and Type-Y[1] [8–11] depending on the Z_2 charge assignment to fermions.

In a CPC 2HDM, one of the three states is identified as the CP-odd Higgs boson which does not couple to the gauge bosons. In a CPV 2HDM, however, all three neutral Higgs states are mixed, one of which is identified with the 125 GeV Higgs bosons and all have non-zero Higgs-gauge-gauge type interactions. One of the features of the CPV 2HDMs, then, is the mixing of the three neutral Higgs bosons. CPV 2HDMs have previously been studied in the literature (for early literature see [7, 12] and references therein). Recently, in [13–16] model-independent approaches to CPV 2HDMs have been presented using the CP-odd weak-basis invariants. Charged Higgs phenomenology in CPV 2HDMs has been considered in [17, 19–23]. Surviving regions of the parameter space passing all experimental constraints in CPV 2HDMs have been studied in [24–28] and in [29] with a focus on EW Baryogenesis. Search signals for explicit CPV have been suggested for Z_2 symmetric 2HDMs in [30, 31] and for the general 2HDM in [32].

In the present paper, we provide a dedicated analysis of CPV in Type-I 2HDMs, which updates and extends the discussions so far in the literature, including all the relevant constraints and LHC predictions. We study explicit CPV in the case of a 2HDM with a softly-broken Z_2 symmetry where there is only one relevant complex parameter, namely λ_5.[2] The imaginary part of λ_5 is constrained by Electric Dipole Moment (EDM) experiments, by EWPD, by unitarity and by vacuum stability constraints. We take into account all these constraints and parametrise CPV in the model in terms of the imaginary part of λ_5. We especially focus on the Type-I Yukawa interaction, where only one of the Higgs doublets couples to fermions and the extra Higgs boson couplings to fermions are suppressed by $1/\tan\beta$, where $\tan\beta$ is the ratio of two Vacuum Expectation Values (VEVs) of the two Higgs doublets. However, the extra Higgs bosons decays to W^+W^- and ZZ can be enhanced with large $\tan\beta$ due to suppressed decays to a fermion pair when the value of mixing angles and mass eigenvalues of the neutral Higgs states are fixed. In other 2HDM types, some Yukawa couplings are proportional to $\tan\beta$ which leads to dominant fermion-pair decays of the neutral Higgses and could hide the W^+W^- and ZZ decay modes. Moreover, in the Type-I 2HDM, extra Higgs boson contributions to EDMs are suppressed in the large $\tan\beta$ regime and mainly the modified couplings of the SM-like Higgs boson contribute to EDMs. We present LHC signatures for observing CPV in this model. Of immediate interest to the LHC is the golden channel where all three neutral Higgs bosons are observed to decay into weak gauge boson pairs, i.e., W^+W^- and ZZ, providing a smoking gun signature of CPV 2HDMs (since purely CP-odd Higgs states cannot decay in these modes). In summary, we perform a dedicated study of the CPV Type-I 2HDM where we take into account the latest experimental and theoretical bounds and present the

[1] The Type-X and Type-Y 2HDMs are also referred to as the lepton-specific and flipped 2HDMs, respectively [7].

[2] The imaginary part of the soft symmetry breaking term, μ_3^2, can be written in terms of the imaginary part of λ_5.

gauge couplings and Branching Ratios (BRs) of the neutral and charged Higgs bosons, the ratio of decay rates of the SM-like Higgs boson and Higgs signal strengths.

The remainder of this paper is organised as follows. In section 2 we present the scalar potential in Z_2-symmetric 2HDMs and the mass spectra in their CPC and CPV limits. In section 3 we show the Yukawa and kinetic Lagrangian in the CPV limit of the Type-I model. In section 4.1 we show the constraints imposed on the model and present four sets of parameters (mass spectra) allowed by these constraints for different values of $\tan\beta$ and $\sin(\beta-\tilde{\alpha})$ ($\tilde{\alpha}$ being a mixing parameter). In the remainder of section 4 we show the gauge couplings and Branching Ratios (BRs) of the neutral and charged Higgs bosons, the ratio of decay rates of the SM Higgs boson and Higgs signal strengths in this model. We recap our results and draw our conclusions in section 5.

2 The scalar potential

The most general 2HDM potential is of the following form:

$$\begin{aligned} V^{\text{gen}} &= \mu_1^2(\phi_1^\dagger\phi_1) + \mu_2^2(\phi_2^\dagger\phi_2) - \left[\mu_3^2(\phi_1^\dagger\phi_2) + \text{h.c.}\right] \\ &\quad + \frac{1}{2}\lambda_1(\phi_1^\dagger\phi_1)^2 + \frac{1}{2}\lambda_2(\phi_2^\dagger\phi_2)^2 + \lambda_3(\phi_1^\dagger\phi_1)(\phi_2^\dagger\phi_2) + \lambda_4(\phi_1^\dagger\phi_2)(\phi_2^\dagger\phi_1) \\ &\quad + \left[\frac{1}{2}\lambda_5(\phi_1^\dagger\phi_2)^2 + \lambda_6(\phi_1^\dagger\phi_1)(\phi_1^\dagger\phi_2) + \lambda_7(\phi_2^\dagger\phi_2)(\phi_1^\dagger\phi_2) + \text{h.c.}\right]. \end{aligned} \tag{2.1}$$

In general, the scalar doublets are defined as

$$\phi_1 = \begin{pmatrix} \phi_1^+ \\ \frac{v_1+h_1^0+ia_1^0}{\sqrt{2}} \end{pmatrix}, \quad \phi_2 = \begin{pmatrix} \phi_2^+ \\ \frac{v_2+h_2^0+ia_2^0}{\sqrt{2}} \end{pmatrix}, \tag{2.2}$$

where v_1 and v_2 could in principle be complex.

In the general case, the 2HDMs suffer from the appearance of FCNCs at the tree level which are strongly restricted experimentally. It is known that imposing a Z_2 symmetry, which can be softly-broken in general, on the scalar potential and extending it to the fermion sector could forbid these FCNCs. Depending on the Z_2 charge assignment for fermions, four independent types of Yukawa interactions are allowed. We will discuss the types of Yukawa interactions in section 3. In the following, the transformations of two Higgs doublets under Z_2 are fixed to be $\phi_1 \to +\phi_1$ and $\phi_2 \to -\phi_2$.

Imposing the softly-broken Z_2 symmetry on the potential reduces it to

$$\begin{aligned} V &= \mu_1^2(\phi_1^\dagger\phi_1) + \mu_2^2(\phi_2^\dagger\phi_2) - \left[\mu_3^2(\phi_1^\dagger\phi_2) + \text{h.c.}\right] + \frac{1}{2}\lambda_1(\phi_1^\dagger\phi_1)^2 + \frac{1}{2}\lambda_2(\phi_2^\dagger\phi_2)^2 \\ &\quad + \lambda_3(\phi_1^\dagger\phi_1)(\phi_2^\dagger\phi_2) + \lambda_4(\phi_1^\dagger\phi_2)(\phi_2^\dagger\phi_1) + \frac{1}{2}\left[\lambda_5(\phi_1^\dagger\phi_2)^2 + \text{h.c.}\right], \end{aligned} \tag{2.3}$$

where μ_3^2 and λ_5 are complex and the rest of the parameters in the potential are real. In the presence of an exact Z_2 symmetry, using the *rephasing invariance* of [33], the phases of the v_i's in eq. (2.2) can be removed by a redefinition of μ_3^2 and λ_5 and so, henceforth, one can not introduce spontaneous CPV. However, in the case a softly broken Z_2 symmetry, spontaneous CPV can occur when $\mathrm{Im}(\lambda_5^*[\mu_3^2]^2) = 0$ and there exist no basis in which λ_5, μ_3^2 and the VEVs are real.

In this paper, we take the VEVs to be real and positive and study explicit CPV which occurs when $\mathrm{Im}(\lambda_5^*[\mu_3^2]^2) \neq 0$ [12, 34]. We then define the VEV related to the Fermi constant G_F as $v^2 \equiv v_1^2 + v_2^2 = (\sqrt{2}G_F)^{-1} \simeq (246\,\mathrm{GeV})^2$ and the ratio of the two VEVs to be $\tan\beta = v_2/v_1$. Thus, the only source of CPV in this model is explicit CPV through the complex parameters:

$$\mu_3^2 = \mathrm{Re}\mu_3^2 + i\mathrm{Im}\mu_3^2, \quad \text{and} \quad \lambda_5 = \mathrm{Re}\lambda_5 + i\mathrm{Im}\lambda_5. \tag{2.4}$$

In what follows we will be using the notation below

$$\mathrm{Re}\lambda_5 \equiv \lambda_5^r, \qquad \mathrm{Im}\lambda_5 \equiv \lambda_5^i. \tag{2.5}$$

2.1 Minimising the potential

The tadpole conditions for the potential,

$$\left.\frac{\partial V}{\partial h_1^0}\right|_0 = 0, \quad \left.\frac{\partial V}{\partial h_2^0}\right|_0 = 0, \quad \left.\frac{\partial V}{\partial a_1^0}\right|_0 = 0, \tag{2.6}$$

where one gets the same results for a_2^0 as for a_1^0, lead to the following equations

$$\begin{aligned} \mu_1^2 - \mathrm{Re}\mu_3^2\ \tan\beta + \frac{v^2}{2}(\lambda_1\ c_\beta^2 + \lambda_{345}\ s_\beta^2) &= 0, \\ \mu_2^2 - \mathrm{Re}\mu_3^2\ \cot\beta + \frac{v^2}{2}(\lambda_2\ s_\beta^2) + \lambda_{345}\ c_\beta^2) &= 0, \\ \mathrm{Im}\mu_3^2 - \frac{v^2}{2}\lambda_5^i\ s_\beta\ c_\beta &= 0, \end{aligned} \tag{2.7}$$

where

$$\lambda_{345} \equiv \lambda_3 + \lambda_4 + \lambda_5^r. \tag{2.8}$$

We introduced the abbreviations such that $s_\theta = \sin\theta$, $c_\theta = \cos\theta$ and $t_\theta = \tan\theta$ and will use them henceforth. Using the first two relations in eq. (2.7), we can eliminate μ_1^2 and μ_2^2 from the potential. The third relation determines $\mathrm{Im}\mu_3^2$ in terms of other parameters,

$$\mathrm{Im}\mu_3^2 = \frac{v^2}{2}\lambda_5^i s_\beta c_\beta. \tag{2.9}$$

Then λ_5^i may be regarded as the only source of CPV. We introduce the "soft breaking scale" of the Z_2 symmetry,

$$M^2 = \frac{\mathrm{Re}\mu_3^2}{s_\beta\ c_\beta}. \tag{2.10}$$

It is also useful to introduce the so-called Higgs basis to express the mass matrices for the scalar bosons, where we can separate the Nambu-Goldstone (NG) boson states from the physical ones. In the Higgs basis [35], the rotated doublets are represented by $\hat{\phi}_i$ and are defined as

$$\begin{pmatrix} \hat{\phi}_1 \\ \hat{\phi}_2 \end{pmatrix} = \begin{pmatrix} c_\beta & s_\beta \\ -s_\beta & c_\beta \end{pmatrix} \begin{pmatrix} \phi_1 \\ \phi_2 \end{pmatrix}, \tag{2.11}$$

where

$$\hat{\phi}_1 = \begin{pmatrix} G^+ \\ \frac{v+h'_1+iG^0}{\sqrt{2}} \end{pmatrix}, \quad \hat{\phi}_2 = \begin{pmatrix} H^+ \\ \frac{h'_2+ih'_3}{\sqrt{2}} \end{pmatrix}, \tag{2.12}$$

with $G^\pm$ and G^0 being the NG bosons absorbed into the longitudinal components of the W and Z bosons, respectively.

The mass of the charged Higgs states, $H^\pm$, is calculated to be

$$m_{H^\pm}^2 = M^2 - \frac{v^2}{2}(\lambda_4 + \lambda_5^r). \tag{2.13}$$

The mass matrix for the three neutral states is given by the 3×3 form in the Higgs basis (h'_1, h'_2, h'_3) as

$$\mathcal{M}^2 = \begin{pmatrix} v^2(\lambda_1 c_\beta^4 + \lambda_2 s_\beta^4 + \frac{1}{2}\lambda_{345} s_{2\beta}^2) & \frac{v^2}{2} s_{2\beta}(\lambda_2 s_\beta^2 - \lambda_1 c_\beta^2 + c_{2\beta}\lambda_{345}) & -\frac{v^2}{2}\lambda_5^i s_{2\beta} \\ \frac{v^2}{2} s_{2\beta}(\lambda_2 s_\beta^2 - \lambda_1 c_\beta^2 + c_{2\beta}\lambda_{345}) & M^2 + v^2 s_\beta^2 c_\beta^2(\lambda_1 + \lambda_2 - 2\lambda_{345}) & -\frac{v^2}{2}\lambda_5^i c_{2\beta} \\ -\frac{v^2}{2}\lambda_5^i s_{2\beta} & -\frac{v^2}{2}\lambda_5^i c_{2\beta} & M^2 - v^2\lambda_5^r \end{pmatrix}. \tag{2.14}$$

This matrix is diagonalised by introducing the 3×3 orthogonal matrix R as

$$\begin{pmatrix} h'_1 \\ h'_2 \\ h'_3 \end{pmatrix} = R \begin{pmatrix} H_1 \\ H_2 \\ H_3 \end{pmatrix}, \quad R^T \mathcal{M}^2 R = \mathcal{M}^2_{\text{diag}} = \text{diag}(m_{H_1}^2, m_{H_2}^2, m_{H_3}^2), \tag{2.15}$$

where H_1, H_2 and H_3 represent the mass eigenstates whereas $m_{H_1}^2$, $m_{H_2}^2$ and $m_{H_3}^2$ ($m_{H_1} \leq m_{H_2} \leq m_{H_3}$ is assumed by definition) are corresponding squared masses. In the following, we identify H_1 as the SM-like Higgs boson, so that we take $m_{H_1} = 125\,\text{GeV}$, and the notations H_1 and h will be used interchangeably.

The scalar three point couplings are calculated from the Higgs potential. The trilinear neutral Higgs boson couplings can be extracted in the following way:

$$\begin{aligned} \mathcal{L} &= \lambda_{ijk} h'_i h'_j h'_k + \cdots \qquad (2.16) \\ &= \lambda_{ijk} \sum_{\alpha=1}^{3} \sum_{\beta=1}^{3} \sum_{\gamma=1}^{3} R_{i\alpha} R_{j\beta} R_{k\gamma} H_\alpha H_\beta H_\gamma + \cdots \\ &= \lambda_{abc} H_a H_b H_c + \cdots, \qquad (2.17) \end{aligned}$$

where H_a are the mass eigenstates of the neutral Higgs boson and

$$\lambda_{abc} = \sum_{i,j,k=1}^{3} \lambda_{ijk} [R_{ia} R_{jb} R_{kc} + (\text{independent permutations of } a,\, b \text{ and } c)]. \tag{2.18}$$

The analytic expressions for λ_{ijk} and the $H^+ H^- H_a$ couplings are given in appendix A.

2.1.1 The $\lambda_5^i = 0$ limit

Since λ_5^i is the only source of CPV in our model, taking the limit of $\lambda_5^i \to 0$ reduces the model to the CPC 2HDM. In this limit, the mass matrix for the neutral Higgs bosons, $\mathcal{M}^2$ in eq. (2.14), becomes the block-diagonal form with the 2×2 part and the 1×1 part where the former corresponds to the mass matrix for the CP-even Higgs states and the latter to the squared mass of the CP-odd Higgs state. The two CP-even states and one CP-odd state can respectively be denoted as $(h,\ H)\,(= H_1,\ H_2)$ and $A\,(= H_3)$ which is the usual notation in the literature on the CPC 2HDMs.

The mass matrix for the CP-even Higgs bosons is diagonalised by the angle $\beta - \alpha$ as

$$t_{2(\beta-\alpha)} = \frac{2\mathcal{M}_{12}^2}{\mathcal{M}_{22}^2 - \mathcal{M}_{11}^2}, \tag{2.19}$$

with the mass squared eigenvalues,

$$m_h^2 = \mathcal{M}_{11}^2 s_{\beta-\alpha}^2 + \mathcal{M}_{22}^2 c_{\beta-\alpha}^2 - \mathcal{M}_{12}^2 s_{2(\beta-\alpha)}, \tag{2.20}$$

$$m_H^2 = \mathcal{M}_{11}^2 c_{\beta-\alpha}^2 + \mathcal{M}_{22}^2 s_{\beta-\alpha}^2 + \mathcal{M}_{12}^2 s_{2(\beta-\alpha)}. \tag{2.21}$$

The relation between the Higgs basis (h_1', h_2') and the mass eigenstate basis (h, H) is then given by

$$\begin{pmatrix} h_1' \\ h_2' \end{pmatrix} = \begin{pmatrix} s_{\beta-\alpha} & c_{\beta-\alpha} \\ c_{\beta-\alpha} & -s_{\beta-\alpha} \end{pmatrix} \begin{pmatrix} h \\ H \end{pmatrix}, \tag{2.22}$$

with $0 \le \beta \le \pi/2$. The squared mass of A is given by

$$m_A^2 = \mathcal{M}_{33}^2. \tag{2.23}$$

2.1.2 The $\lambda_5^i \ll 1$ case

Note that the parameter λ_5^i in eq. (2.14), appearing in the off-diagonal elements in the third row and third column, is tightly constrained by EDM bounds as they will be discussed in section 4.1. Therefore, we study the model in the $\lambda_5^i \ll 1$ case where $\mathcal{M}_{\text{block}}^2$ is (upper 2×2) block diagonal.

$$\mathcal{R}^T \mathcal{M}^2 \mathcal{R} = \mathcal{M}_{\text{block}}^2 + \mathcal{O}\left((\lambda_5^i)^2\right), \tag{2.24}$$

where the rotation matrix above is

$$\mathcal{R} = \begin{pmatrix} 1 & 0 & 0 \\ 0 & c_{23} & -s_{23} \\ 0 & s_{23} & c_{23} \end{pmatrix} \begin{pmatrix} c_{13} & 0 & -s_{13} \\ 0 & 1 & 0 \\ s_{13} & 0 & c_{13} \end{pmatrix} = \begin{pmatrix} c_{13} & 0 & -s_{13} \\ -s_{13}s_{23} & c_{23} & -c_{13}s_{23} \\ c_{23}s_{13} & s_{23} & c_{13}c_{23} \end{pmatrix}, \tag{2.25}$$

where c_{ij} and s_{ij} are $\cos(\alpha_{ij})$ and $\sin(\alpha_{ij})$, respectively (with $ij = 13$ or 23). In principle, we allow for

$$-\frac{\pi}{2} < \alpha_{23} \le \frac{\pi}{2}, \quad -\frac{\pi}{2} < \alpha_{13} \le \frac{\pi}{2}, \tag{2.26}$$

and the mixing angles can be expressed as

$$t_{23} = \frac{s_{23}}{c_{23}} = \frac{v^2\left(\mathcal{M}_{11}^2 - \mathcal{M}_{33}^2 - \mathcal{M}_{12}^2\, t_{2\beta}\right)\, \lambda_5^i\, c_{2\beta}}{2\mathcal{M}_{12}^2 - 2\left(\mathcal{M}_{11}^2 - \mathcal{M}_{33}^2\right)\left(\mathcal{M}_{22}^2 - \mathcal{M}_{33}^2\right)} + \mathcal{O}\left((\lambda_5^i)^2\right), \tag{2.27}$$

$$t_{13} = \frac{s_{13}}{c_{13}} = \frac{-v^2\, c_{23}\, s_{2\beta}\lambda_5^i - 2\, c_{2\beta}^2 \mathcal{M}_{12}^2\, s_{23}}{2c_{2\beta}^2\left(\mathcal{M}_{11}^2 - \mathcal{M}_{33}^2\, c_{23}^2\right)} + \mathcal{O}\left((\lambda_5^i)^2\right). \tag{2.28}$$

Therefore, by neglecting the $\mathcal{O}\left((\lambda_5^i)^2\right)$ contribution, the mass squared matrix is diagonalised by

$$\begin{aligned} \mathcal{M}_{\text{diag}}^2 &= R^T \mathcal{M}^2 R \\ &= R_{\beta-\alpha}^T \mathcal{R}^T \mathcal{M}^2 \mathcal{R} R_{\beta-\alpha} \\ &\simeq R_{\beta-\alpha}^T\, \mathcal{M}_{\text{block}}^2\, R_{\beta-\alpha}, \end{aligned} \tag{2.29}$$

where the upper block is diagonalised in a similar way to eq. (2.22), as

$$R_{\beta-\alpha} = \begin{pmatrix} s_{\beta-\alpha} & c_{\beta-\alpha} & 0 \\ c_{\beta-\alpha} & -s_{\beta-\alpha} & 0 \\ 0 & 0 & 1 \end{pmatrix}. \tag{2.30}$$

Using the above expression, we obtain the approximate expression for the diagonalisation matrix R:

$$R \simeq \begin{pmatrix} s_{\beta-\alpha} & c_{\beta-\alpha} & -s_{13} \\ c_{\beta-\alpha} & -s_{\beta-\alpha} & -s_{23} \\ s_{13} + s_{23}c_{\beta-\alpha} & s_{13}c_{\beta-\alpha} - s_{13}s_{\beta-\alpha} & 1 \end{pmatrix}. \tag{2.31}$$

As described in subsection 2.1.1, we can define the SM-like limit by taking $\lambda_5^i = 0$ (equivalently $s_{13} = s_{23} = 0$) and $s_{\beta-\alpha} = 1$, where H_1 has the same Yukawa and gauge couplings as those of the SM Higgs boson.

Therefore, the 9 independent parameters in the model,

$$\mu_1^2,\ \mu_2^2,\ \mathrm{Re}\,\mu_3^2,\quad \lambda_1,\ \lambda_2,\ \lambda_3,\ \lambda_4,\ \lambda_5^r,\ \lambda_5^i. \tag{2.32}$$

can be re-expressed in terms of the following parameters which we shall use as inputs:

$$v,\ \tilde{m}_h,\ \tilde{m}_H,\ \tilde{m}_A,\ m_{H^\pm},\ \tan\beta,\ s_{\beta-\tilde{\alpha}},\ M^2,\ \lambda_5^i, \tag{2.33}$$

where the parameters with tilde are defined as

$$\tilde{m}_h^2 \equiv \mathcal{M}_{11}^2 s_{\beta-\tilde{\alpha}}^2 + \mathcal{M}_{22}^2 c_{\beta-\tilde{\alpha}}^2 - \mathcal{M}_{12}^2 s_{2(\beta-\tilde{\alpha})}, \tag{2.34}$$

$$\tilde{m}_H^2 \equiv \mathcal{M}_{11}^2 c_{\beta-\tilde{\alpha}}^2 + \mathcal{M}_{22}^2 s_{\beta-\tilde{\alpha}}^2 + \mathcal{M}_{12}^2 s_{2(\beta-\tilde{\alpha})}, \tag{2.35}$$

$$t_{2(\beta-\tilde{\alpha})} \equiv \frac{2\mathcal{M}_{12}^2}{\mathcal{M}_{22}^2 - \mathcal{M}_{11}^2}, \tag{2.36}$$

$$\tilde{m}_A^2 \equiv \mathcal{M}_{33}^2. \tag{2.37}$$

	Φ_1	Φ_2	u_R	d_R	e_R	Q_L, L_L	ξ_u	ξ_d	ξ_e
Type-I	$+$	$-$	$-$	$-$	$-$	$+$	$\cot\beta$	$\cot\beta$	$\cot\beta$
Type-II	$+$	$-$	$-$	$+$	$+$	$+$	$\cot\beta$	$-\tan\beta$	$-\tan\beta$
Type-X	$+$	$-$	$-$	$-$	$+$	$+$	$\cot\beta$	$\cot\beta$	$-\tan\beta$
Type-Y	$+$	$-$	$-$	$+$	$-$	$+$	$\cot\beta$	$-\tan\beta$	$\cot\beta$

Table 1. Z_2 charge assignment in the four types of Yukawa interactions and the ξ_f factor in each of types.

We note that in the CPC limit, $\tilde{m}_h$, $\tilde{m}_H$ and $\tilde{m}_A$ correspond to the masses of the two CP-even and one CP-odd Higgs bosons, respectively, and $\beta - \tilde{\alpha}$ is the mixing angle which diagonalises the CP-even Higgs states in the Higgs basis (see eqs. (2.19), (2.20) and (2.21)).

The relation between $m_h(= 125$ GeV) and $\tilde{m}_h$ is described using the parameters defined in eqs. (2.34)–(2.36) as

$$m_h^2 = \tilde{m}_h^2 c_\chi^2 + \tilde{m}_A^2 s_\chi^2 - \frac{v^2}{2}\lambda_5^i[s_{2\beta}s_{\beta-\tilde{\alpha}} + c_{2\beta}c_{\beta-\tilde{\alpha}}]s_{2\chi}, \tag{2.38}$$

with

$$\tan 2\chi = \frac{v^2\lambda_5^i}{\tilde{m}_A^2 - \tilde{m}_h^2}s_{2\beta}. \tag{2.39}$$

In the numerical evaluation, the value of $\tilde{m}_h$ is varied so as to reproduce 125 GeV.

3 The Yukawa and kinetic Lagrangian

The most general form of the Yukawa Lagrangian under the introduced Z_2 symmetry is given by

$$-\mathcal{L}_Y = Y_u\overline{Q}_L i\sigma_2\phi_u^* u_R + Y_d\overline{Q}_L\phi_d d_R + Y_e\overline{L}_L\phi_e e_R + \text{h.c.}, \tag{3.1}$$

where $\phi_{u,d,e}$ are ϕ_1 or ϕ_2 depending on the type of Yukawa interaction. When we specify the Z_2 charge assignment for fermions as given in table 1, $\phi_{u,d,e}$ are determined. For example, in the Type-II 2HDM $\phi_d = \phi_e = \phi_1$ and $\phi_u = \phi_2$. The interaction terms are expressed as

$$\begin{aligned}-\mathcal{L}_Y^{\text{int}} = &\sum_{f=u,d,e}\frac{m_f}{v}\sum_{i=1,2,3}\left(\xi_f^{H_i}\overline{f}fH_i - 2i\,I_f\tilde{\xi}_f^{H_i}\overline{f}\gamma_5 fH_i\right)\\ &+\frac{\sqrt{2}}{v}\Big[V_{ud}\overline{u}\left(m_d\xi_d P_R - m_u\xi_u P_L\right)d\,H^+ + m_e\xi_e\overline{\nu}P_R eH^+ + \text{h.c.}\Big],\end{aligned} \tag{3.2}$$

where I_f is the third component of the isospin for a fermion f and the ξ_f values are listed in table 1. In eq. (3.2), the coefficients for the scalar (pseudo-scalar) type couplings $\xi_f^{H_i}$

$(\tilde{\xi}_f^{H_i})$ are given by

$$\xi_f^{H_1} = R_{11} + \xi_f R_{21} \simeq s_{\beta-\alpha} + \xi_f c_{\beta-\alpha}, \tag{3.3}$$
$$\xi_f^{H_2} = R_{12} + \xi_f R_{22} \simeq c_{\beta-\alpha} - \xi_f s_{\beta-\alpha}, \tag{3.4}$$
$$\xi_f^{H_3} = R_{13} + \xi_f R_{23} \simeq -s_{13} - s_{23}\xi_f, \tag{3.5}$$
$$\tilde{\xi}_f^{H_1} = \xi_f R_{31} \simeq \xi_f(s_{13} + s_{23}c_{\beta-\alpha}), \tag{3.6}$$
$$\tilde{\xi}_f^{H_2} = \xi_f R_{32} \simeq \xi_f(s_{13}c_{\beta-\alpha} - s_{13}s_{\beta-\alpha}), \tag{3.7}$$
$$\tilde{\xi}_f^{H_3} = \xi_f R_{33} \simeq \xi_f, \tag{3.8}$$

where the approximated formulae given in the above rightmost hand sides are obtained using eq. (2.31) which is valid for the case of $\lambda_5^i \ll 1$.

The kinetic terms for the scalar fields are given by

$$\mathcal{L}_{\rm kin} = |D_\mu\phi_1|^2 + |D_\mu\phi_2|^2 = |D_\mu\hat{\phi}_1|^2 + |D_\mu\hat{\phi}|^2. \tag{3.9}$$

The gauge-gauge-scalar type interactions only appear from the first, $|D_\mu\hat{\phi}_1|^2$. They are extracted as

$$|D_\mu\hat{\phi}_1|^2 = g_{hVV}^{\rm SM}(\xi_V^{H_1}H_1 + \xi_V^{H_2}H_2 + \xi_V^{H_3}H_3)V_\mu V^\mu + \cdots, \quad V_\mu = W_\mu\,, Z_\mu, \tag{3.10}$$

where $g_{hVV}^{\rm SM}$ is the hVV vertex in the SM, and

$$\xi_V^{H_1} = R_{11} \simeq s_{\beta-\alpha}, \tag{3.11}$$
$$\xi_V^{H_2} = R_{12} \simeq c_{\beta-\alpha}, \tag{3.12}$$
$$\xi_V^{H_3} = R_{13} \simeq -s_{\beta-\alpha}s_{13} + c_{\beta-\alpha}s_{23}. \tag{3.13}$$

Note that the alignment limit in which the coupling of $H_1\,(= h)$ are exactly SM-like is achieved in the limit of $\lambda_5^i \to 0$ (equivalently $s_{13} = s_{23} = 0$) and $s_{\beta-\alpha} \to 1$.

Similar to the discussion of the Yukawa couplings, the approximated formulae given in the above rightmost hand sides are obtained using eq. (2.31). The scalar-scalar-gauge type interactions are also extracted from eq. (3.9):

$$\begin{aligned}
|D_\mu\hat{\phi}_2|^2 = &-\frac{g}{2}\Big[(R_{31}+iR_{21})H^+\overleftrightarrow{\partial}_\mu H_1 + (R_{32}+iR_{22})H^+\overleftrightarrow{\partial}_\mu H_2 \\
&\qquad + (R_{33}+iR_{23})H^+\overleftrightarrow{\partial}_\mu H_3\Big]W^{-\mu} + \text{h.c.} \\
&+\frac{g_Z}{2}\Big[(R_{21}R_{32}+R_{22}R_{31})H_1\overleftrightarrow{\partial}_\mu H_2 + (R_{21}R_{33}+R_{23}R_{31})H_1\overleftrightarrow{\partial}_\mu H_3 \\
&\qquad + (R_{22}R_{33}+R_{23}R_{32})H_2\overleftrightarrow{\partial}_\mu H_3\Big]Z^\mu + \cdots,
\end{aligned} \tag{3.14}$$

where $X\overleftrightarrow{\partial}_\mu Y \equiv X(\partial_\mu Y) - Y(\partial_\mu X)$.

4 Numerical results in the Type-I 2HDM with CPV

4.1 Constraints on the parameters

4.1.1 Theoretical bounds

The stability condition for the Higgs potential is given by requiring that the potential be bounded from below in any direction of the scalar boson space. The necessary and sufficient conditions to guarantee such a positivity of the potential are [36]

$$\lambda_1 > 0, \quad \lambda_2 > 0, \quad \sqrt{\lambda_1\lambda_2} + \lambda_3 + \mathrm{MIN}(0,\ \lambda_4 - |\lambda_5|) > 0. \tag{4.1}$$

From the S-matrix unitarity for elastic scattering of 2 body to 2 body bosonic states, the magnitude of combinations of λ parameters in the potential can be constrained. In refs. [37, 38], the diagonalised s-wave amplitude matrix for these scattering processes has been derived in the CPC 2HDM. For the CPV case, we obtain all the eigenvalues of the s-wave amplitude matrix just by replacing λ_5^r with $|\lambda_5| = \sqrt{(\lambda_5^r)^2 + (\lambda_5^i)^2}$ [39, 40].

As for the constraints from experimental data, we take into account EDMs and the S, T and U parameters [41–44]. In particular, the CPV parameter, i.e., λ_5^i can significantly affect EDMs, so its magnitude is constrained. The bounds from the EDM constraints have been discussed in refs. [26, 45] in CPV 2HDMs. In general, there are two sources which contribute to EDMs in CPV 2HDMs, namely, the modified couplings of the SM-like Higgs boson and contributions from additional Higgs bosons. In the Type-I 2HDM, the pseudo-scalar type interaction among the additional Higgs bosons and fermions are suppressed by the factor of $1/\tan\beta$ as we see eq. (3.6) with $\xi_u = \xi_d = \xi_e = \cot\beta$, so that the additional Higgs boson contributions can be neglected in a large $\tan\beta$ regime. In the following, we focus on the Type-I 2HDM and we apply the bound from EDMs in the following way [45]

$$\tilde{\xi}_u^{H_1} \leq 10^{-2}. \tag{4.2}$$

Regarding the S, T and U parameters, we use the following bounds [46] on the deviations in these parameters under the fixed value of $\Delta U = 0$:

$$\Delta S = 0.05 \pm 0.09, \quad \Delta T = 0.08 \pm 0.07, \tag{4.3}$$

where ΔX is the difference between the $X = (S,\ T \text{ or } U)$ parameter in the 2HDM and in the SM. The correlation coefficient of ΔS and ΔT is taken to be $+0.91$.

4.1.2 Experimental bounds

The B physics data also provides constraints on the parameter space in 2HDMs, which are especially sensitive to $m_{H^\pm}$ and $\tan\beta$. A comprehensive study for the constraint on the CPC 2HDMs has been done in ref. [47], where various B physics observables such as $b \to s\gamma$, B^0-$\bar{B}^0$ mixing, $B \to \tau\nu$ have been taken into account. In the CPV 2HDM, the Yukawa couplings of the charged Higgs boson are the same as those of the CPC 2HDMs, therefore we can apply the same bound related to the $H^{\pm}$ mediation as that reported in [47] to the CPV case studied here.[3]

In addition, we also take into account the constraint from direct searches for extra Higgs bosons at the LHC. The search for neutral Higgs bosons decaying into $\tau\tau$ using the LHC Run-I data reported in [49], excludes $\tan\beta \gtrsim 10$ (30) for $m_A = 300$ (700) GeV in the minimal supersymmetric SM. A similar bound is expected in the non-supersymmetric Type-II 2HDM, since the structure of the Yukawa interactions are the same. However, there is no $\tan\beta$ enhancement in the Yukawa couplings in the Type-I 2HDM studied here since the Yukawa couplings are suppressed by the factor of $\cot\beta$. The production cross section is, therefore, suppressed by $\cot^2\beta$. As a result, since we do not consider the case of $\tan\beta \ll 1$, our model satisfies the constraint from the direct searches at the LHC.

There are also constraints from the $A \to Zh$ process [50] which we need to take into account. The upper limit on the $\sigma(gg \to A) \times \mathrm{BR}(A \to Zh) \times \mathrm{BR}(h \to f\bar{f})$ has been given in the region of $m_A = 220$-$1000\,\mathrm{GeV}$ using the LHC Run-I data. For $f = \tau\,(b)$, the upper limit is measured to be $0.098 - 0.013$ pb ($0.57 - 0.014$ pb). In our model, the typical cross section of $gg \to H_{2,3}$ is of order 1 pb in the case of $m_{H_{2,3}} = 200\,\mathrm{GeV}$ and $\tan\beta \gtrsim 2$, and the branching fraction of the $A \to Zh$ mode is less than order of 10^{-2}. On the other hand, the decay rate of the SM-like Higgs boson does not change so much from the SM prediction, so that the branching fraction of $h \to \tau\tau(b\bar{b})$ is $\sim 7\%(60\%)$. Therefore, our prediction of the cross section is well below the upper limit.

In figure 1, we show the allowed parameter regions on the λ_5^i and $\tan\beta$ plane from the EDMs given by eq. (4.2) and the S and T parameters given by eq. (4.3). We take $\tilde{m}_H = 200\,\mathrm{GeV}$, $\tilde{m}_A = m_{H^{\pm}}$ and $s_{\beta-\tilde{\alpha}} = 1$. The mass of the charged Higgs boson $m_{H^{\pm}}$ is taken to be 250, 300, 400 and 700 GeV. We note that the bounds from the EDMs and the S and T parameters do not depend on the value of M^2. Although the M^2 dependence appears in the constraints from the unitarity and vacuum stability, these bounds can be avoided by taking an appropriate value of M^2 for each fixed value of $\tan\beta$ and λ_5^i. We confirmed that the case for $m_{H^{\pm}} \gtrsim 750\,\mathrm{GeV}$ is excluded by unitarity bounds.[4]

Because the masses of neutral Higgs bosons are derived as output, we show m_{H_2} and m_{H_3} as a function of λ_5^i in figure 2. As we explained in subsection 2.1.2, the mass of the SM-like Higgs boson m_{H_1} is kept to be 125 GeV by taking an appropriate value of $\tilde{m}_h$ for each fixed values of the input parameters. In this figure, we take the same set of input parameters as in figure 1. We see that for the case with $\lambda_5^i \lesssim 0.1$, $m_{H_2} \simeq \tilde{m}_H$ and $m_{H_3} \simeq \tilde{m}_A$ are given. However, when we take a larger value of λ_5^i, the above approximate relations are broken due to the CP-mixing effect. This behaviour is getting more significant when we take a smaller value of $m_{H^{\pm}}$. As it will become clear later, what is important to note now is the fact that m_{H2} and m_{H_3} are never degenerate.

[3] In ref. [48], the BaBar Collaboration has reported that the measured ratios $\mathrm{BR}(B \to D^*\tau\nu)/\mathrm{BR}(B \to D^*\ell\nu)$ and $\mathrm{BR}(B \to D\tau\nu)/\mathrm{BR}(B \to D\ell\nu)$ ($\ell = e, \mu$) deviate from the SM predictions by 2.7σ and 2.0σ, respectively, and their combined deviation is 3.4σ. These deviations cannot be simultaneously compensated by a natural flavor conserving version such as a Z_2 symmetric 2HDMs with and without CPV.

[4] Note that this upper limit on $m_{H^{\pm}}$ is due to the assumption that the masses of other scalars are relatively close. If one takes the decoupling limit into account, the mass of the charged scalar could be arbitrarily high without violating any unitarity limits.

JHEP04(2016)048

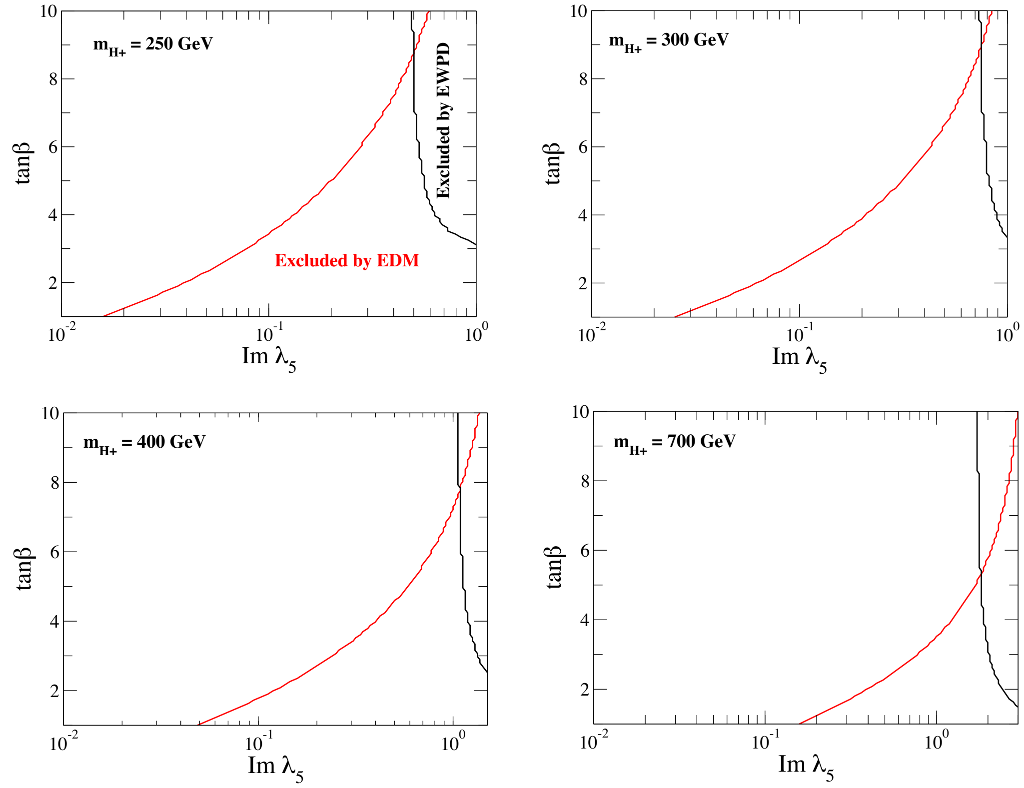

Figure 1. The constrained region in the λ_5^i-$\tan\beta$ plane is shown in the case of $\tilde{m}_H = 200\,\text{GeV}$, $\tilde{m}_A = m_{H^\pm}$ and $s_{\beta-\tilde{\alpha}} = 1$. The upper-left, upper-right, lower-left and lower-right panels respectively show the case of $m_{H^\pm} = 250$, 300, 400 and 700 GeV. For all the panels, the right regions from the red and black curves are excluded by the EDM and the electroweak S and T parameters bounds, respectively.

In figure 3, we show the excluded parameter space due to EDMs and the S and T parameters in the λ_5^i-$s_{\beta-\tilde{\alpha}}$ plane for different values of $\tan\beta$, namely, $\tan\beta = 2$ (left panel), 5 (center panel) and 10 (right panel). In these plots, we take $\tilde{m}_H = 200\,\text{GeV}$ and $\tilde{m}_A = m_{H^\pm} = 250\,\text{GeV}$.

4.2 Phenomenology at the LHC

For our numerical results, we use the fixed input parameters $\tilde{m}_H = 200\,\text{GeV}$ and $\tilde{m}_A = m_{H^\pm} = 250\,\text{GeV}$ which correspond to the case shown in the upper-left panel of figures 1–2 and in figure 3.

For the calculations of decay rates of the Higgs bosons, it is important to show the value of gauge-gauge-scalar type couplings which are described by $g_{hVV}^{\text{SM}} \times \xi_V^{H_i}$ $(i = 1, 2, 3)$ given in eqs. (3.11)–(3.13). We thus first show the values of $\xi_V^{H_i}$ as a function of λ_5^i in figure 4. In this plot, $\tan\beta$ is fixed to be 5 (left panels) and 10 (right panels). The value of $s_{\beta-\tilde{\alpha}}$ is taken to be 1 in the upper panels and 0.98 in the lower panels, in compliance with LHC data. The vertical dotted line shows the upper limit on λ_5^i from the EDMs and S and T parameters. It is evident that, over the λ_5^i allowed regions, deviations of the SM-like Higgs couplings to W^+W^- and ZZ pairs induced by CPV are negligible, thereby generating no

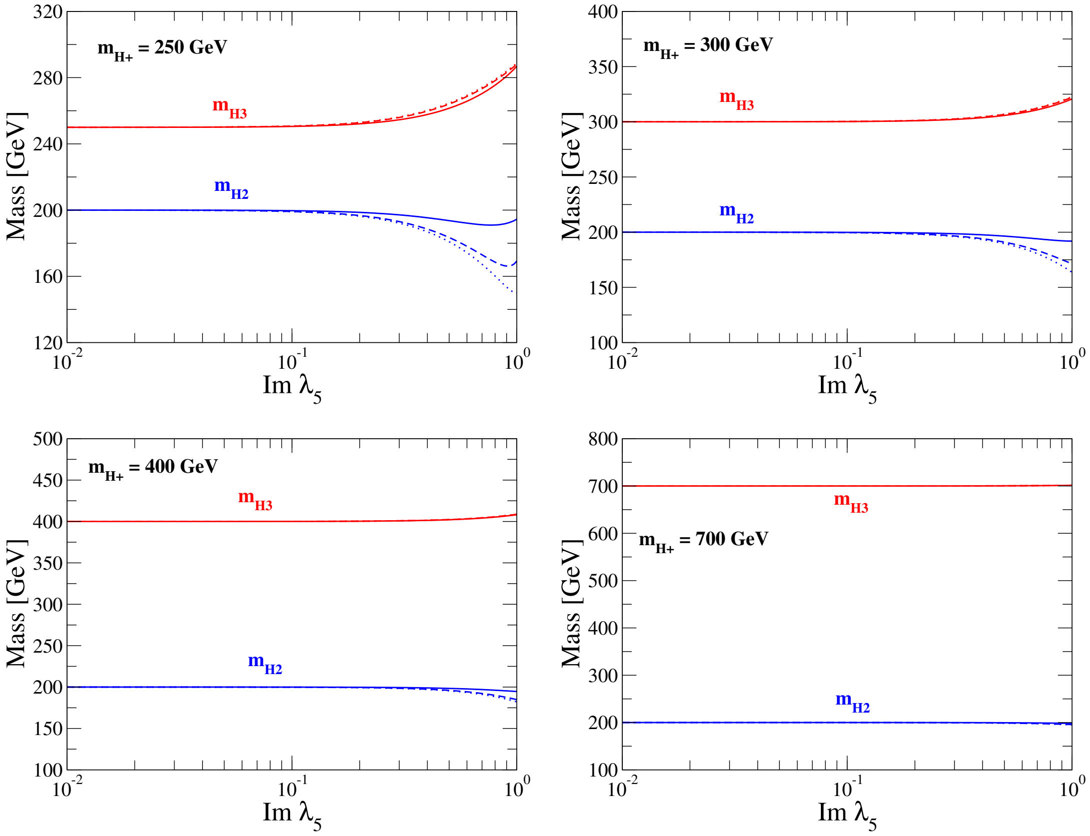

Figure 2. The masses of H_2 and H_3 as a function of λ_5^i. We take the same parameter set as in figure 1. The mass of the SM-like Higgs boson H_1 is kept to be 125 GeV. In each plot the solid, dashed and dotted curves correspond to $\tan\beta = 2$, 5 and 10, respectively.

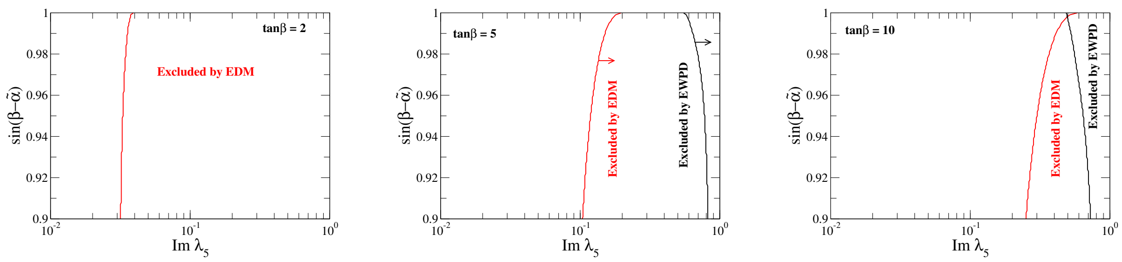

Figure 3. The constrained region in the λ_5^i-$s_{\beta-\tilde{\alpha}}$ plane is shown in the case of $\tilde{m}_H = 200$ GeV and $\tilde{m}_A = m_{H^\pm} = 250$ GeV. The left, center and right panels show the case of $\tan\beta = 2$, 5 and 10, respectively. For all the panels, the right regions from the red and black curves are excluded by the EDMs and the S and T parameters bounds, respectively.

tension against LHC data. On the other hand, the magnitudes of corresponding couplings of the other two neutral Higgs states, H_2 and H_3, grow with increasing λ_5^i. Note that $|\xi_V^{H_2}|$ increases rapidly as $s_{\beta-\tilde{\alpha}}$ changes from 1 to 0.98, while it does not change considerably with the change in $\tan\beta$. However, $|\xi_V^{H_3}|$ decreases with growing $\tan\beta$ and with the change of $s_{\beta-\tilde{\alpha}}$ from 1 to 0.98. This is clearly conducive to establish the W^+W^- and ZZ decays of three Higgs states of the 2HDM Type-I we are considering as a hallmark signature of CPV.

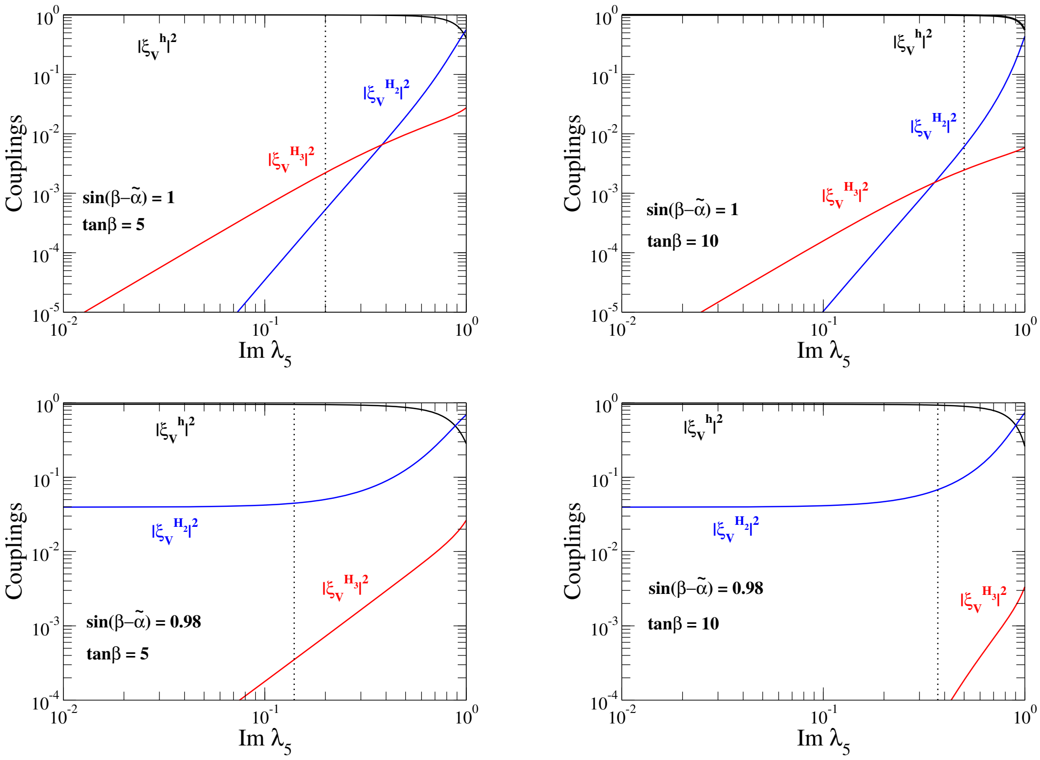

Figure 4. The coefficient of the gauge-gauge-scalar type couplings for $h(= H_1)$, H_2 and H_3 defined in eqs. (3.11), (3.12) and (3.13), respectively, as a function of λ_5^i for $\tan\beta = 5$ (left) and $\tan\beta = 10$ (right). The value of $s_{\beta-\tilde{\alpha}}$ is taken to be 1 in the upper panels and 0.98 in the lower panels. For all the plots, we take $\tilde{m}_H = 200\,\text{GeV}$ and $\tilde{m}_A = m_{H^\pm} = 250\,\text{GeV}$. The vertical dotted line shows the upper limit on λ_5^i from the EDMs and S and T parameters.

In figure 5, we present the ratio of decay rates of the H_1 (identified as the h, the SM-like Higgs boson) to those of $h_{\rm SM}$ (the Higgs boson in the SM) for two values of $\tan\beta = 5$ (on the left) and $\tan\beta = 10$ (on the right). The vertical dotted line as usual shows the upper limit on λ_5^i. Over the allowed λ_5^i intervals, none of BRs of the SM-like Higgs boson of our 2HDM Type-I deviates significantly from the LHC data, with the possible exception of $b\bar{b}, \tau^+\tau^-$ and gg, when $s_{\beta-\tilde{\alpha}}$ departs from 1 at small $\tan\beta$. This effect may thus be significant in order to establish CPV in our scenario in cases where the H_1 state is not produced in the SM-like channels presently investigated and constrained by the LHC, for example, in cascade decays of the heavier Higgs states. We remark though that this occurs in a complementary region of 2HDM Type-I parameter space to the one where treble W^+W^- and ZZ signals of the neutral Higgs states can be established, i.e., when $s_{\beta-\tilde{\alpha}}$ is closer to 1 and $\tan\beta$ is larger.

Figure 6 shows the signal strength, μ_{XY}, of the SM-like Higgs boson $h(= H_1)$, defined as

$$\mu_{XY} = \frac{\sigma(gg \to H_1)}{\sigma(gg \to h_{\rm SM})} \times \frac{{\rm BR}(H_1 \to XY)}{{\rm BR}(h_{\rm SM} \to XY)}, \quad XY = W^+W^-,\ ZZ,\ gg,\ \gamma\gamma,\ Z\gamma,\ \tau^+\tau^-, \tag{4.4}$$

$$\mu_{b\bar{b}} = \frac{\sigma(q\bar{q} \to H_1 V)}{\sigma(q\bar{q} \to h_{\rm SM} V)} \times \frac{{\rm BR}(H_1 \to b\bar{b})}{{\rm BR}(h_{\rm SM} \to b\bar{b})}. \tag{4.5}$$

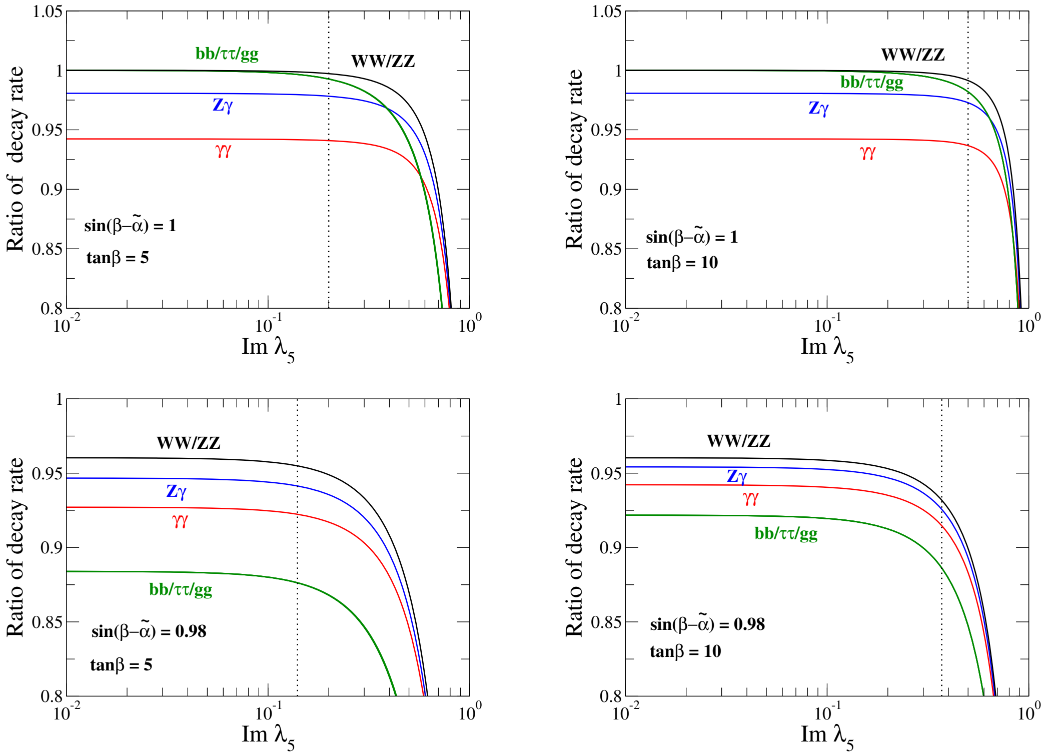

Figure 5. The ratio of decay rates of $h(= H_1)$ to those of the SM Higgs boson $h_{\rm SM}$ as a function of λ_5^i for $\tan\beta = 5$ (on the left) and $\tan\beta = 10$ (on the right). The values of $s_{\beta-\tilde{\alpha}}$ are taken to be 1 and 0.98 for the upper and lower panels, respectively. For all the plots, we take $\tilde{m}_H = 200\,$GeV and $\tilde{m}_A = m_{H^\pm} = 250\,$GeV. The vertical dotted line shows the upper limit on λ_5^i from the EDMs and S and T parameters. We take M =190 and 180 GeV for the cases of $s_{\beta-\tilde{\alpha}} = 1$ and 0.98, respectively.

Owing to the interplay between the CPV effects entering directly or indirectly the signal strengths via the production cross sections, partial decay widths and the total one as seen at the LHC, of the three aforementioned decay modes of the H_1 state, only the $\tau^+\tau^-$ one may carry some evidence of CPV effects, again, for the same conditions, i.e., when $s_{\beta-\tilde{\alpha}}$ departs from 1 at small $\tan\beta$. Hence, this offers a second handle to access CPV in the 2HDM Type-I studied here, alternative to the smoking gun signature of the aforementioned W^+W^- and ZZ decays, as the measurements of the fermionic signal strengths of the SM-like Higgs state will improve at Run 2 of the LHC.

Figure 7 shows the BRs of the second lightest neutral Higgs boson, H_2, as a function of λ_5^i for $\tan\beta = 5$ (on the left) and $\tan\beta = 10$ (on the right). We take $s_{\beta-\tilde{\alpha}} = 1$ (upper panels) and 0.98 (lower panels). Similarly, figure 8 does so for the heaviest neutral Higgs boson, H_3. By contrasting the two, it is evident that the largest W^+W^- and ZZ rates are *simultaneously* found, as intimated, for large $\tan\beta$ and H_1 couplings very SM-like. Note that $H_1, H_2, H_3 \to WW/ZZ$ are all large simultaneously only in the upper top plot of figures 7–8 already well below the EDM limit, whereas in the other 3 plots this decay rate can be large only very close to the EDM limit (in the top left plot, $H_2 \to WW/ZZ$

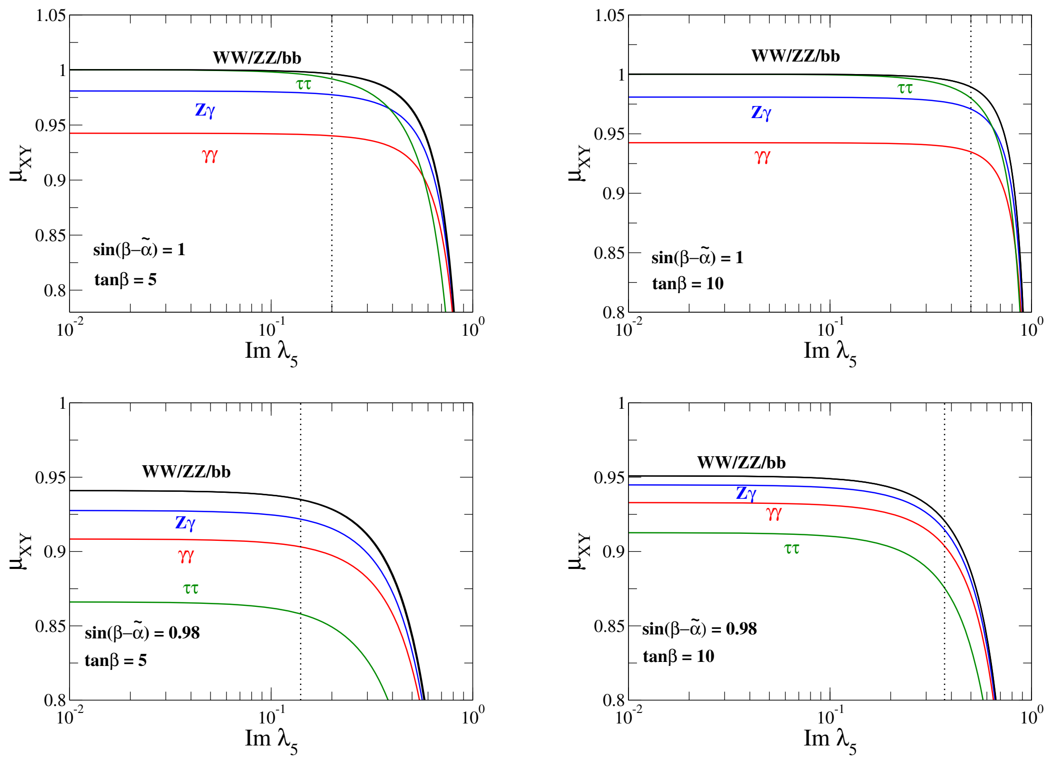

Figure 6. The signal strength for the SM-like Higgs boson $h(= H_1)$ as a function of λ_5^i for $\tan\beta = 5$ (on the left) and $\tan\beta = 10$ (on the right). The values of $s_{\beta-\tilde{\alpha}}$ are taken to be 1 and 0.98 for the upper and lower panels, respectively. For all the plots, we take $\tilde{m}_H = 200\,\text{GeV}$ and $\tilde{m}_A = m_{H^\pm} = 250\,\text{GeV}$. The vertical dotted line shows the upper limit on λ_5^i from the EDMs and S and T parameters. We take M =190 and 180 GeV for the cases of $s_{\beta-\tilde{\alpha}} = 1$ and 0.98, respectively.

becomes dominant essentially where the parameter space is starting to be ruled out) or else only 2 of the channels can be large at the same (in the bottom plots, $H_3 \to WW/ZZ$ is always subleading). Another possible hallmark signal of CPV could be the hZ one, having assessed that current experimental constraints force the $H_1 \equiv h$ state of the 2HDM Type-I to be essentially CP-even. Under this condition, in fact, to establish hZ, it would mean for both H_2 and H_3 to have a CP-odd nature, hence unlike the case of the corresponding CPC version of our scenario. Unfortunately, the H_2 and H_3 BRs are never large simultaneously in the allowed λ_5^i regions. As for other decay modes, while interesting patterns emerge, we notice that none of these can be taken as a direct evidence of CPV as they all exist already in the CPC case for both the heavy Higgs states.

Figure 9 shows the BRs of the charged Higgs bosons, $H^\pm$, as a function of λ_5^i for $\tan\beta = 5$ (on the left) and $\tan\beta = 10$ (on the right). As usual, we take $s_{\beta-\tilde{\alpha}} = 1$ (upper panels) and 0.98 (lower panels). As just remarked for most of the H_2 and H_3 decay rates, here, again, interesting decay patterns emerge, yet all the possible final states already exist in the CPC case of the 2HDM Type-I. This also includes the case of $hW^\pm$ and $H_2W^\pm$ decays (in the CPC 2HDM Type-I the latter would be either $HW^\pm$ or $AW^\pm$), which show

JHEP04(2016)048

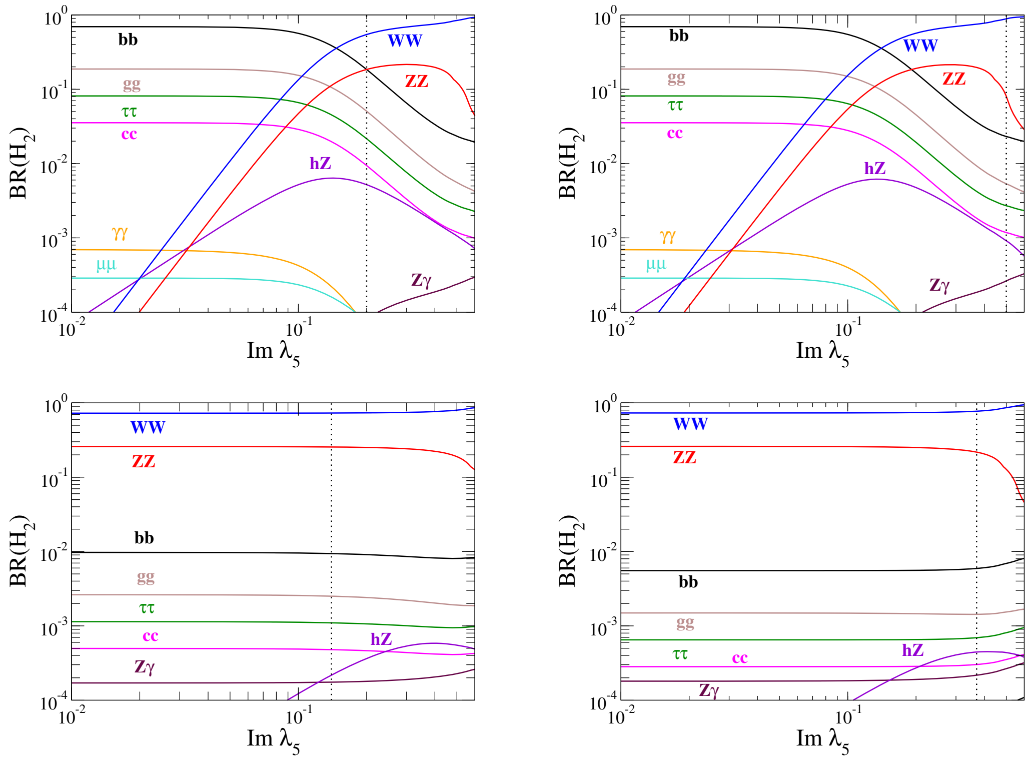

Figure 7. The branching fractions for H_2 as a function of λ_5^i for $\tan\beta = 5$ (on the left) and $\tan\beta = 10$ (on the right). The values of $s_{\beta-\tilde{\alpha}}$ are taken to be 1 and 0.98 for the upper and lower panels, respectively. For all the plots, we take $\tilde{m}_H = 200\,\text{GeV}$ and $\tilde{m}_A = m_{H^\pm} = 250\,\text{GeV}$. The vertical dotted line shows the upper limit on λ_5^i from the EDMs and S and T parameters. We take M =190 and 180 GeV for the cases of $s_{\beta-\tilde{\alpha}} = 1$ and 0.98, respectively.

	$\sigma(gg \to H_2)$	$\sigma(gg \to H_3)$	$\sigma(gb \to H^\pm t)$	$pp \to H_2 H_3$	$pp \to H_2 H^\pm$	$pp \to H_3 H^\pm$	$pp \to H^+ H^-$
$t_\beta = 5$	0.79(0.90)	4.22(4.83)	0.057(0.070)	9.0(10)$\times10^{-3}$	18(21)$\times10^{-3}$	12(14)$\times10^{-3}$	6.9(7.9)$\times10^{-3}$
$t_\beta = 10$	0.20(0.23)	1.06(1.22)	0.014(0.018)	8.9(10)$\times10^{-3}$	18(21)$\times10^{-3}$	12(14)$\times10^{-3}$	6.9(7.9)$\times10^{-3}$

Table 2. Production cross sections (in the unit of pb) for extra Higgs bosons at the LHC with the collision energy of 13 (14) TeV in the case of $\tan\beta = 5$ and 10. We take $\lambda_5^i = 0.1$, $\tilde{m}_H = 200\,\text{GeV}$, $m_{H^\pm} = \tilde{m}_A = 250\,\text{GeV}$ and $s_{\beta-\tilde{\alpha}} = 1$.

an interesting interplay (as function of λ_5^i) generally unseen in the CPC case, which may eventually help as confirmation of CPV being present in the charged Higgs sector too.

Clearly, in order so see the smoking gun signals described above, one should make sure that H_2, H_3 and $H^\pm$ states of the 2HDM Type-I can be copiously produced at the LHC. Hence, we finally calculate their production cross sections at the LHC. For the neutral Higgs bosons, there are two dominant production processes, namely, the gluon fusion process $gg \to H_2$, H_3 and the pair production $pp \to Z^* \to H_2 H_3$. For the $H^\pm$ case, there are the gb fusion process $gb \to H^\pm t$ and the pair production $pp \to \gamma^*/Z^* \to H^+H^-$. In addition to these processes, there are are also mixed modes, i.e., where neutral and charge Higgs states are produced together via $pp \to W^* \to H^\pm H_2$ and $pp \to W^* \to H^\pm H_3$.

JHEP04(2016)048

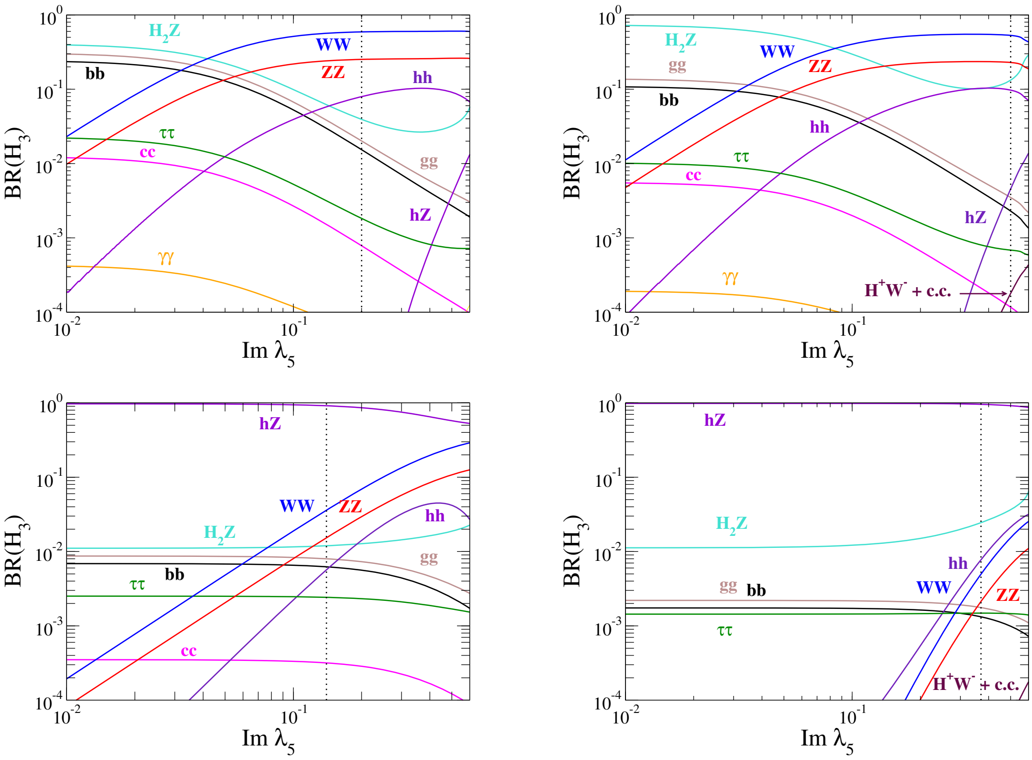

Figure 8. The branching fractions for H_3 as a function of λ_5^i for $\tan\beta = 5$ (on the left) and $\tan\beta = 10$ (on the right). The values of $s_{\beta-\tilde{\alpha}}$ are taken to be 1 and 0.98 for the upper and lower panels, respectively. For all the plots, we take $\tilde{m}_H = 200\,\text{GeV}$ and $\tilde{m}_A = m_{H^\pm} = 250\,\text{GeV}$. The vertical dotted line shows the upper limit on λ_5^i from the EDMs and S and T parameters. We take M =190 and 180 GeV for the cases of $s_{\beta-\tilde{\alpha}} = 1$ and 0.98, respectively.

The cross section of the gluon fusion process is calculated by

$$\sigma(gg \to H_2) = \sigma(gg \to h_{\text{SM}})|_{m_{h_{\text{SM}}}=m_{H_2}} \times \frac{\Gamma(H_2 \to gg)}{\Gamma(h_{\text{SM}} \to gg)}, \tag{4.6}$$

$$\sigma(gg \to H_3) = \sigma(gg \to h_{\text{SM}})|_{m_{h_{\text{SM}}}=m_{H_3}} \times \frac{\Gamma(H_3 \to gg)}{\Gamma(h_{\text{SM}} \to gg)}, \tag{4.7}$$

where $\sigma(gg \to h_{\text{SM}})$ and $\Gamma(h_{\text{SM}} \to gg)$ are the gluon fusion cross section and the decay rate of $h_{\text{SM}} \to gg$ for the SM Higgs boson h_{SM}, respectively. From ref. [51], $\sigma(gg \to h_{\text{SM}})$ is given to be 18.35 pb (21.02 pb) with the collision energy of 13 (14) TeV. For the other processes, we calculate these cross sections ourselves. The results are listed in table 2 with the collision energy of 13 (14) TeV using `CTEQ6L` [52] as Parton Distribution Functions (PDFs) at the scale $\mu = \hat{s}$. We notice that all cross sections are in the $\mathcal{O}(10)$–$\mathcal{O}(1000)$ range, so that the 2HDM Type-I scenario with CPV discussed here would most likely be probed fully in the years to come, if not at the standard LHC already, certainly at the tenfold luminosity increase foreseen at the Super-LHC [53].

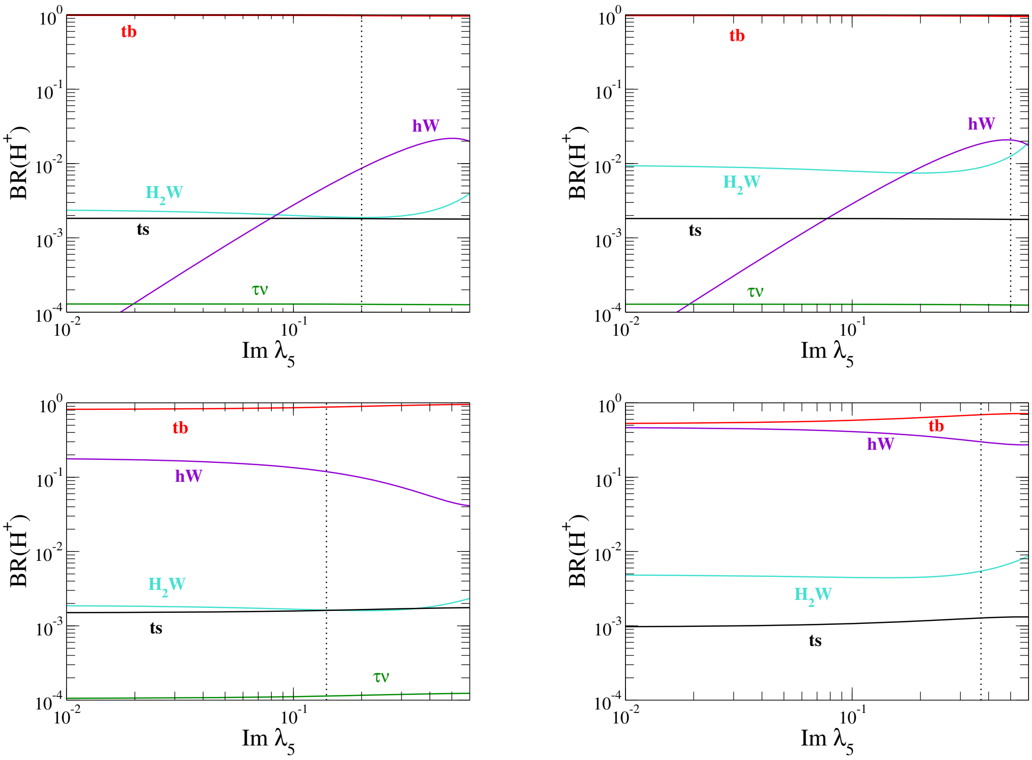

Figure 9. The branching fractions for H_2 as a function of λ_5^i for $\tan\beta = 5$ (on the left) and $\tan\beta = 10$ (on the right). The values of $s_{\beta-\tilde{\alpha}}$ are taken to be 1 and 0.98 for the upper and lower panels, respectively. For all the plots, we take $\tilde{m}_H = 200\,\text{GeV}$ and $\tilde{m}_A = m_{H^\pm} = 250\,\text{GeV}$. The vertical dotted line shows the upper limit on λ_5^i from the EDMs and S and T parameters. We take M =190 and 180 GeV for the cases of $s_{\beta-\tilde{\alpha}} = 1$ and 0.98, respectively.

5 Discussion and conclusion

In this paper we have studied CPV 2HDMs with a softly-broken Z_2 symmetry which is imposed to avoid dangerous FCNCs. We have analysed in detail the constraints (mainly from the EDMs and S, T parameters) and LHC predictions in the Type-I 2HDM in particular.

We have first highlighted possible CPV effects onto the lightest Higgs state of this scenario, H_1. Herein, deviations from the SM-like behaviour induced by CPV in our scenario, being small and indirect, while possibly measurable (in fermionic decays) and interesting per se, may be difficult to interpret as such. In fact, the gold plated smoking gun signature of the CPV 2HDM Type-I is the decay of both H_2 and H_3 into weak gauge boson pairs. Experimentally this will require the observation of all three neutral Higgs bosons $H_{1,2,3}$ decaying into W^+W^- and/or ZZ states. In order to resolve the two heavy neutral Higgs bosons, $H_{2,3}$, they must be sufficiently non-degenerate with a mass splitting greater than say 10 GeV, which we have seen to be realisable in our scenario. For example, for one of the benchmarks considered here, we have $m_{H^\pm} \approx m_{H_3} \approx 250\,\text{GeV}$ and $m_{H_2} \approx 200\,\text{GeV}$, with a mass splitting of about 50 GeV. Further confirmation of the mixed CP-nature of the heavy neutral Higgs states could come from their hZ decays, in presence of a light Higgs

JHEP04(2016)048

state which is essentially SM-like in its quantum numbers, $H_1 \equiv h_{\rm SM}$. As for the charged Higgs sector, indirect evidence of CPV induced by the neutral Higgs states could be seen in the interplay between $H^\pm \to hW^\pm$ and $H_2W^\pm$ decays.

The production cross sections of all heavy states H_2, H_3 and $H^\pm$ must also be sufficiently large, which we have shown to possibly be the case if both the standard and high luminosity conditions of the LHC are considered.

In summary, the 2HDM Type-I is a framework which can implement explicit CPV effects at tree level, free from both theoretical flaws and experimental constraints, that can be probed at the LHC.

Acknowledgments

SFK acknowledges partial support from the STFC Consolidated Grant ST/J000396/ 1 and European Union FP7 ITN-INVISIBLES (Marie Curie Actions, PITN-GA-2011-289442). SM is financed in part through the NExT Institute and from the STFC Consolidated Grant ST/ J000396/1. He also acknowledges the H2020-MSCA-RICE-2014 grant no. 645722 (NonMinimalHiggs). VK's research is financially supported by the Academy of Finland project "The Higgs Boson and the Cosmos" and project 267842. KY is supported by a JSPS postdoctoral fellowships for research abroad.

A Higgs trilinear couplings

The trilinear neutral Higgs boson couplings λ_{ijk} defined in eq. (2.16) are given by

$$\lambda_{333} = \lambda_{223} = -\frac{1}{3}\lambda_{113} = \frac{v}{4}\lambda_5^i \sin 2\beta, \tag{A.1}$$

$$\lambda_{123} = -\, v\lambda_5^i \cos 2\beta, \tag{A.2}$$

$$\lambda_{222} = \lambda_{233} = \frac{v}{8}\left[\lambda_2 - \lambda_1 + (\lambda_1 + \lambda_2 - 2\lambda_{345})\cos 2\beta\right]\sin 2\beta, \tag{A.3}$$

$$\lambda_{112} = -\,\frac{3v}{8}\left[\lambda_1 - \lambda_2 + (\lambda_1 + \lambda_2 - 2\lambda_{345})\cos 2\beta\right]\sin 2\beta, \tag{A.4}$$

$$\lambda_{111} = \frac{v}{16}\left[3(\lambda_1 + \lambda_2) + 2\lambda_{345} + 4(\lambda_1 - \lambda_2)\cos 2\beta + (\lambda_1 + \lambda_2 - 2\lambda_{345})\cos 4\beta\right], \tag{A.5}$$

$$\lambda_{122} = \frac{v}{16}\left[3(\lambda_1 + \lambda_2) + 2\lambda_{345} - 3(\lambda_1 + \lambda_2 - 2\lambda_{345})\cos 4\beta\right], \tag{A.6}$$

$$\lambda_{133} = \frac{v}{16}\left[\lambda_1 + \lambda_2 + 16(\lambda_3 + \lambda_4) - 10\lambda_{345} - (\lambda_1 + \lambda_2 - 2\lambda_{345})\cos 4\beta\right]. \tag{A.7}$$

The $h_1'H^+H^-$ and $h_2'H^+H^-$ couplings are given by

$$\lambda_{h_1'H^+H^-} = \frac{v}{8}\left[\lambda_1 + \lambda_2 + 8\lambda_3 - 2\lambda_{345} - (\lambda_1 + \lambda_2 - 2\lambda_{345})c_{4\beta}\right], \tag{A.8}$$

$$\lambda_{h_2'H^+H^-} = \frac{v}{4}s_{2\beta}\left[-\lambda_1 + \lambda_2 + (\lambda_1 + \lambda_2 - 2\lambda_{345})c_{2\beta}\right]. \tag{A.9}$$

References

[1] ATLAS collaboration, *Observation of a new particle in the search for the standard model Higgs boson with the ATLAS detector at the LHC*, Phys. Lett. **B 716** (2012) 1 [arXiv:1207.7214] [INSPIRE].

[2] CMS collaboration, *Observation of a new boson at a mass of* 125 GeV *with the CMS experiment at the LHC*, Phys. Lett. **B 716** (2012) 30 [arXiv:1207.7235] [INSPIRE].

[3] A.D. Sakharov, *Violation of CP invariance, c asymmetry and baryon asymmetry of the universe*, Pisma Zh. Eksp. Teor. Fiz. **5** (1967) 32 [*JETP Lett.* **5** (1967) 24] [*Sov. Phys. Usp.* **34** (1991) 392] [*Usp. Fiz. Nauk* **161** (1991) 61] [INSPIRE].

[4] V.A. Kuzmin, V.A. Rubakov and M.E. Shaposhnikov, *On the anomalous electroweak baryon number nonconservation in the early universe*, Phys. Lett. **B 155** (1985) 36 [INSPIRE].

[5] J.F. Gunion and H.E. Haber, *The CP conserving two Higgs doublet model: the approach to the decoupling limit*, Phys. Rev. **D 67** (2003) 075019 [hep-ph/0207010] [INSPIRE].

[6] J.F. Gunion, H.E. Haber, G.L. Kane and S. Dawson, *The Higgs hunter's guide*, *Front. Phys.* **80** (2000) 1 [INSPIRE].

[7] G.C. Branco et al., *Theory and phenomenology of two-Higgs-doublet models*, Phys. Rept. **516** (2012) 1 [arXiv:1106.0034] [INSPIRE].

[8] V.D. Barger, J.L. Hewett and R.J.N. Phillips, *New constraints on the charged Higgs sector in two Higgs doublet models*, Phys. Rev. **D 41** (1990) 3421 [INSPIRE].

[9] Y. Grossman, *Phenomenology of models with more than two Higgs doublets*, Nucl. Phys. **B 426** (1994) 355 [hep-ph/9401311] [INSPIRE].

[10] A.G. Akeroyd, *Nonminimal neutral Higgs bosons at LEP-2*, Phys. Lett. **B 377** (1996) 95 [hep-ph/9603445] [INSPIRE].

[11] M. Aoki, S. Kanemura, K. Tsumura and K. Yagyu, *Models of Yukawa interaction in the two Higgs doublet model and their collider phenomenology*, Phys. Rev. **D 80** (2009) 015017 [arXiv:0902.4665] [INSPIRE].

[12] H.E. Haber and D. O'Neil, *Basis-independent methods for the two-Higgs-doublet model. II. The significance of* $\tan\beta$, Phys. Rev. **D 74** (2006) 015018 [hep-ph/0602242] [INSPIRE].

[13] D. Sokolowska, K.A. Kanishev and M. Krawczyk, *On distinguishing the direct and spontaneous CP-violation in 2HDM*, PoS(CHARGED2008)016 [arXiv:0812.0296] [INSPIRE].

[14] B. Grzadkowski, O.M. Ogreid and P. Osland, *Measuring CP-violation in two-Higgs-doublet models in light of the LHC Higgs data*, JHEP **11** (2014) 084 [arXiv:1409.7265] [INSPIRE].

[15] B. Grzadkowski, O.M. Ogreid and P. Osland, *Diagnosing CP properties of the 2HDM*, JHEP **01** (2014) 105 [arXiv:1309.6229] [INSPIRE].

[16] B. Grzadkowski, O.M. Ogreid and P. Osland, *Testing the presence of CP-violation in the 2HDM*, PoS(CORFU2014)086 [arXiv:1504.06076] [INSPIRE].

[17] M. Jung, A. Pich and P. Tuzon, *Charged-Higgs phenomenology in the aligned two-Higgs-doublet model*, JHEP **11** (2010) 003 [arXiv:1006.0470] [INSPIRE].

[18] A. Pich and P. Tuzon, *Yukawa alignment in the two-Higgs-doublet model*, Phys. Rev. **D 80** (2009) 091702 [arXiv:0908.1554] [INSPIRE].

[19] A. Arhrib, E. Christova, H. Eberl and E. Ginina, *CP violation in charged Higgs production and decays in the complex two Higgs doublet model*, JHEP **04** (2011) 089 [arXiv:1011.6560] [INSPIRE].

JHEP04(2016)048

[20] S.-S. Bao, Y. Tang and Y.-L. Wu, *$W^{\pm}H^{\mp}$ associated production at LHC in the general 2HDM with spontaneous CP-violation*, Phys. Rev. **D 83** (2011) 075006 [arXiv:1011.1409] [INSPIRE].

[21] L. Basso et al., *Probing the charged Higgs boson at the LHC in the CP-violating type-II 2HDM*, JHEP **11** (2012) 011 [arXiv:1205.6569] [INSPIRE].

[22] L. Basso et al., *The CP-violating type-II 2HDM and charged Higgs boson benchmarks*, arXiv:1305.3219 [INSPIRE].

[23] W. Mader, J.-h. Park, G.M. Pruna, D. Stöckinger and A. Straessner, *LHC explores what LEP hinted at: CP-violating type-I 2HDM*, JHEP **09** (2012) 125 [*Erratum ibid.* **1401** (2014) 006] [arXiv:1205.2692] [INSPIRE].

[24] M. Jung and A. Pich, *Electric dipole moments in two-Higgs-doublet models*, JHEP **04** (2014) 076 [arXiv:1308.6283] [INSPIRE].

[25] J. Brod, U. Haisch and J. Zupan, *Constraints on CP-violating Higgs couplings to the third generation*, JHEP **11** (2013) 180 [arXiv:1310.1385] [INSPIRE].

[26] S. Inoue, M.J. Ramsey-Musolf and Y. Zhang, *CP-violating phenomenology of flavor conserving two Higgs doublet models*, Phys. Rev. **D 89** (2014) 115023 [arXiv:1403.4257] [INSPIRE].

[27] R. Gaitan, E.A. Garces, J.H.M. de Oca and R. Martinez, *Top quark chromoelectric and chromomagnetic dipole moments in a two Higgs doublet model with CP-violation*, Phys. Rev. **D 92** (2015) 094025 [arXiv:1505.04168] [INSPIRE].

[28] C.-Y. Chen, S. Dawson and Y. Zhang, *Complementarity of LHC and EDMs for exploring Higgs CP-violation*, JHEP **06** (2015) 056 [arXiv:1503.01114] [INSPIRE].

[29] S. Ipek, *Perturbative analysis of the electron electric dipole moment and CP-violation in two-Higgs-doublet models*, Phys. Rev. **D 89** (2014) 073012 [arXiv:1310.6790] [INSPIRE].

[30] A. Barroso, P.M. Ferreira, R. Santos and J.P. Silva, *Probing the scalar-pseudoscalar mixing in the 125 GeV Higgs particle with current data*, Phys. Rev. **D 86** (2012) 015022 [arXiv:1205.4247] [INSPIRE].

[31] D. Fontes, J.C. Romão, R. Santos and J.P. Silva, *Undoubtable signs of CP-violation in Higgs boson decays at the LHC run 2*, Phys. Rev. **D 92** (2015) 055014 [arXiv:1506.06755] [INSPIRE].

[32] L. Diaz-Cruz, A. Diaz-Furlong, R. Gaitan-Lozano and J.H. M. d.O. Y, *Probing flavor changing neutral currents and CP-violation through the decay $h \to c^{-}b^{+}W^{-}$ in the two Higgs doublet model*, arXiv:1203.6893 [INSPIRE].

[33] I.F. Ginzburg and M. Krawczyk, *Symmetries of two Higgs doublet model and CP-violation*, Phys. Rev. **D 72** (2005) 115013 [hep-ph/0408011] [INSPIRE].

[34] H.E. Haber and O. Stål, *New LHC benchmarks for the CP-conserving two-Higgs-doublet model*, Eur. Phys. J. **C 75** (2015) 491 [arXiv:1507.04281] [INSPIRE].

[35] S. Davidson and H.E. Haber, *Basis-independent methods for the two-Higgs-doublet model*, Phys. Rev. **D 72** (2005) 035004 [*Erratum ibid.* **D 72** (2005) 099902] [hep-ph/0504050] [INSPIRE].

[36] B. Grzadkowski, O.M. Ogreid and P. Osland, *Natural multi-Higgs model with dark matter and CP-violation*, Phys. Rev. **D 80** (2009) 055013 [arXiv:0904.2173] [INSPIRE].

[37] S. Kanemura, T. Kubota and E. Takasugi, *Lee-Quigg-Thacker bounds for Higgs boson masses in a two doublet model*, Phys. Lett. **B 313** (1993) 155 [hep-ph/9303263] [INSPIRE].

JHEP04(2016)048

[38] A.G. Akeroyd, A. Arhrib and E.-M. Naimi, *Note on tree level unitarity in the general two Higgs doublet model*, *Phys. Lett.* **B 490** (2000) 119 [hep-ph/0006035] [INSPIRE].

[39] I.F. Ginzburg and I.P. Ivanov, *Tree-level unitarity constraints in the most general 2HDM*, *Phys. Rev.* **D 72** (2005) 115010 [hep-ph/0508020] [INSPIRE].

[40] S. Kanemura and K. Yagyu, *Unitarity bound in the most general two Higgs doublet model*, *Phys. Lett.* **B 751** (2015) 289 [arXiv:1509.06060] [INSPIRE].

[41] M.E. Peskin and T. Takeuchi, *A new constraint on a strongly interacting Higgs sector*, *Phys. Rev. Lett.* **65** (1990) 964 [INSPIRE].

[42] M.E. Peskin and T. Takeuchi, *Estimation of oblique electroweak corrections*, *Phys. Rev.* **D 46** (1992) 381 [INSPIRE].

[43] M.E. Peskin and J.D. Wells, *How can a heavy Higgs boson be consistent with the precision electroweak measurements?*, *Phys. Rev.* **D 64** (2001) 093003 [hep-ph/0101342] [INSPIRE].

[44] H.E. Haber and D. O'Neil, *Basis-independent methods for the two-Higgs-doublet model III: the CP-conserving limit, custodial symmetry and the oblique parameters S, T, U*, *Phys. Rev.* **D 83** (2011) 055017 [arXiv:1011.6188] [INSPIRE].

[45] K. Cheung, J.S. Lee, E. Senaha and P.-Y. Tseng, *Confronting higgcision with electric dipole moments*, *JHEP* **06** (2014) 149 [arXiv:1403.4775] [INSPIRE].

[46] M. Baak et al., *The electroweak fit of the standard model after the discovery of a new boson at the LHC*, *Eur. Phys. J.* **C 72** (2012) 2205 [arXiv:1209.2716] [INSPIRE].

[47] F. Mahmoudi and O. Stål, *Flavor constraints on the two-Higgs-doublet model with general Yukawa couplings*, *Phys. Rev.* **D 81** (2010) 035016 [arXiv:0907.1791] [INSPIRE].

[48] BaBar collaboration, J.P. Lees et al., *Evidence for an excess of $\bar{B} \to D^{(*)}\tau^-\bar{\nu}_\tau$ decays*, *Phys. Rev. Lett.* **109** (2012) 101802 [arXiv:1205.5442] [INSPIRE].

[49] ATLAS collaboration, *Search for neutral Higgs bosons of the minimal supersymmetric standard model in pp collisions at $\sqrt{s} = 8$ TeV with the ATLAS detector*, *JHEP* **11** (2014) 056 [arXiv:1409.6064] [INSPIRE].

[50] ATLAS collaboration, *Search for a CP-odd Higgs boson decaying to Zh in pp collisions at $\sqrt{s} = 8$ TeV with the ATLAS detector*, *Phys. Lett.* **B 744** (2015) 163 [arXiv:1502.04478] [INSPIRE].

[51] https://twiki.cern.ch/twiki/bin/view/LHCPhysics/CERNYellowReportPageAt1314TeV.

[52] J. Pumplin, D.R. Stump, J. Huston, H.L. Lai, P.M. Nadolsky and W.K. Tung, *New generation of parton distributions with uncertainties from global QCD analysis*, *JHEP* **07** (2002) 012 [hep-ph/0201195] [INSPIRE].

[53] F. Gianotti et al., *Physics potential and experimental challenges of the LHC luminosity upgrade*, *Eur. Phys. J.* **C 39** (2005) 293 [hep-ph/0204087] [INSPIRE].

JHEP04(2016)048